JEAP

ISSN: 2525-815X

Journal of Environmental Analysis and Progress

10.24221/jeap.9.4.2024.6499.325-339

Estimating tree aboveground biomass in an Atlantic Forest remnant using different modeling methods

Felipe Zuñe[a], Pablo José Francisco Pena Rodrigues[b], Nílber Gonçalves da Silva[a], Consuelo Rojas-Idrogo[c], Guillermo Eduardo Delgado-Paredes[c], Alex Enrich-Prast[d,e], Cássia Mônica Sakuragui[e]

[a] Universidade Federal do Rio de Janeiro-UFRJ, Museu Nacional, Programa de Pós-Graduação em Ciências Biológicas (Botânica). Horto Botânico, Quinta da Boa Vista, s/n, São Cristóvão, Rio de Janeiro, Rio de Janeiro, Brasil. CEP: 20940-040. E-mail: zunefelipe@gmail.com, nilber@mn.ufrj.br.

[b] Instituto de Pesquisas Jardim Botânico do Rio de Janeiro-IPJBRJ. Rua Pacheco Leão, n. 915, Jardim Botânico, Rio de Janeiro, Rio de Janeiro, Brasil. CEP: 22460-030. E-mail: pablojfpr@hotmail.com.

[c] Universidad Nacional Pedro Ruiz Gallo-UNPRG, Departamento Académico de Botánica. Calle Juan XXIII, n. 391, Lambayeque, Lambayeque, Perú. Código Postal: 14000. E-mail: crojas@unprg.edu.pe, guidelg2015@yahoo.es.

[d] Linköping University, Department of Thematic Studies, Environmental Change. 581 83, Linköping, Sweden. E-mail: aenrichprast@gmail.com.

[e] UFRJ, Instituto de Biologia. Avenida Carlos Chagas Filho, n. 373, Cidade Universitária, Rio de Janeiro, Rio de Janeiro, Brasil. CEP: 21941-901. E-mail: cmsakura12@gmail.com (Corresponding Author).

ARTICLE INFO

Received 05 Dec 2023
Accepted 09 Dec 2024
Published 16 Dec 2024

ABSTRACT

The Atlantic Forest stores vast amounts of aboveground biomass (AGB), yet estimating these stocks is still challenging. We aimed to predict the AGB stock of the largest biodiversity remnant of Serra da Tiririca State Park (Rio de Janeiro, Brazil) by comparing the accuracy of generalized linear models (GLM) and random forest (RF) models. The results derived from field plots showed an AGB of 371 t.ha^{-1}. The comparison between the modeling methods revealed that the GLM is more accurate; still, the RF is also fit to estimate the AGB of the remnant. The most accurate GLM predicted an AGB of 405 t.ha^{-1}. We observed that the accuracy of the models improved when all predictor variables were combined. This study allowed us to improve the AGB estimates and produce an AGB map useful for managing and conserving the remnants.

Keywords: Generalized linear model, random forest, remote sensing.

Introduction

Tropical forests are essential in the global terrestrial carbon cycle (Houghton, 2005). Their large carbon pools, stored as aboveground biomass (AGB), provide numerous ecosystem services and help mitigate greenhouse gases (GHG) (Pan et al., 2011; Pooter et al., 2016; Mitchard, 2018). However, in recent decades an increase in anthropogenic activities, such as deforestation and changes in land use, is responsible for a significant decrease in AGB in tropical forests (Hansen et al., 2013). Large Brazilian biomes, such as the Atlantic Forest, have lost almost 90% of their original coverage (SOS Mata Atlântica & INPE, 2019). It is also known that habitat fragmentation and the consequent loss of biodiversity are strongly related to the decline in AGB (Laurance et al., 2018). Therefore, it is vital to carry out studies that help explain the ecological processes that determine the spatial distribution patterns of AGB (Chave et al., 2019). This is especially true when working in a biome such as the Atlantic Forest, a biodiversity hotspot (Myers et al., 2000) but lacks AGB estimates for most areas (Alves et al., 2010).

Several ecological studies aimed at understanding forest dynamics are based on robust AGB estimates (e.g., Saatchi et al., 2011a; Avitabile et al., 2016; Meira-Junior et al., 2020). However, accurately quantifying AGB stocks requires traditional field sampling methods (Saatchi et al., 2011b). These methods can be destructive, where trees are uprooted and their additive components separated, or non-destructive, where the AGB of trees is estimated from allometric equations and relates diameter, height, and wood density variables (Chave et al., 2014). Although both methods provide accurate AGB information, they are costly, require considerable time, and are not practical for

estimating the spatial distribution of AGB over large areas (Timothy et al., 2016). For this reason, low-cost techniques, such as remote sensing, are increasingly used in AGB estimation studies (Lu et al., 2016).

New approaches in remote sensing allow us to more accurately estimate large AGB stocks (Avitabile et al., 2016). However, remote sensing alone cannot directly determine these stocks, making it necessary to link field information with remote sensing data (Saatchi et al., 2011b). On the other hand, remote sensing data processing is only possible through acquiring aerial or satellite images (Lu, 2005; Santos, Pimentel & Silva, 2023). In this sense, among long-standing space missions, only images from some satellites (e.g., Landsat satellites) have been immensely used in AGB estimate studies (e.g., Powell et al., 2010; Zhu & Liu, 2015; Silveira et al., 2019). This occurs because Landsat images offer comprehensive spatial coverage, are free, and have an intermediate spatial resolution (Goward et al., 2006). Even so, satellite images can be used to explore and extract a wide range of variables needed for the performance of AGB prediction models (Gasparri et al., 2010; Barbosa et al., 2014; Chave et al., 2019).

Improving AGB estimates depends on predictor variables and prediction methods (Lu et al., 2016). In the first case, it is known that numerous variables (e.g., climatic and edaphic) stand out for influencing AGB patterns (Chazdon, 2003; Poorter et al., 2017; Ali et al., 2019). Furthermore, other variables from remote sensing, such as spectral indices and topography, also contribute to a better understanding of the spatial distribution of AGB (Lu et al., 2004; Barbosa et al., 2014; Silveira et al., 2019). For this reason, selecting variables is a fundamental step to ensure the best performance of prediction models (Li et al., 2019). In the second case, several empirical modeling methods estimate AGB (Zhu & Liu, 2015). They range from less detailed scopes, such as linear regressions (Debastiani et al., 2019), to more complex approaches, such as machine learning algorithms (Schuh et al., 2020). Thus, evaluating different modeling methods allows us to maximize the accuracy of AGB predictions (Gagliasso et al., 2014).

Considering the variety of modeling methods, multiple AGB prediction variables, and the fact that improving AGB estimates for the Atlantic Forest is still a challenge, in this study we aimed to: i) evaluate the performance of different modeling methods that predict the AGB, relating field plot AGB information to soil data, remote sensing, and environmental data; and ii) select the most accurate modeling method to generate an AGB map of the remnant.

Material and Methods

Study area

This study was conducted in the coastal remnant of Serra da Tiririca, the principal and largest sector of Serra da Tiririca State Park (PESET) (Rio de Janeiro, 1991). This protected area is 1788.58 ha and is in the municipalities of Maricá and Niterói, in Rio de Janeiro State (22°47'-22°59 S'; 42°57'-43°02' W) (Figure 1). The regional climate is humid and hot, with rainstorms in the summer and a dry season in the winter (Aw climate in the Köppen classification, updated in Alvares et al., 2013). The vegetation type is a dense rainforest (Atlantic Forest) (Barros, 2008). The region has an average annual temperature of 23.7°C, average annual precipitation of 1173 mm, and annual relative humidity of 80%, and the soil is mainly formed by Agrisoils, Cambisols, and Lithosols (INEA, 2015).

Plot data

The field study was carried out between November 2019 and December 2020. In the field, we georeferenced and established ten plots of 50 x 20 m (1 ha) at random (Figure 1) and at least 200 m apart. We marked all living trees within each plot with a diameter at breast height (DBH) ≥ 10 cm and recorded their height (estimated from the length of a pruning pole) and diameter. For the subsequent quantification of wood density and estimation of the trees' AGB, wood samples were extracted from the trees and measured following the Chave (2006) protocol. The tree species recorded in this study can be found in Zuñe-da-Silva et al. (2023).

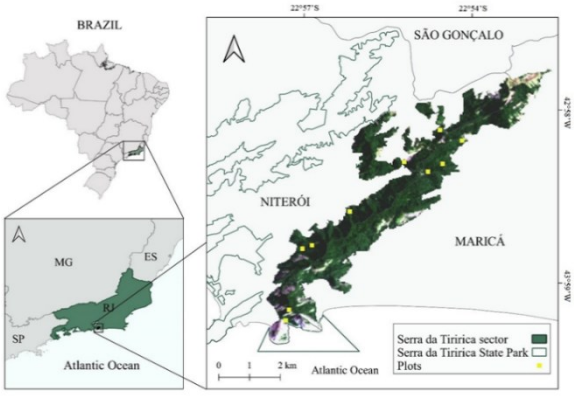

Figure 1. Map of the study area and location of plots installed between 2019 and 2020 in Serra da Tiririca, Rio de Janeiro, Brazil. Font: Zuñe et al. (2024).

Additionally, we collected a soil sample in the center of each plot (between 0 and 20 cm deep). The samples were bagged, labeled, and sent to the Unidade Multiusuário de Análises Ambientais (UMAA) at the Universidade Federal do Rio de Janeiro, where they were processed and analyzed according to EMBRAPA (1997) protocols. The properties evaluated were the following: nitrogen (N), phosphorus (P), organic carbon (C), organic matter (OM), and granulometric fractions of gravel, sand, silt, and clay. Using the Brazilian System of Soil Classification (SiBCS), the soil was classified according to the granulometric texture (EMBRAPA, 2018).

After drying the wood samples in an oven at 105 ± 2°C, we obtained the wood density through immersion (ABNT, 2003). Wood density was calculated using Equation 1.

$$\rho = \frac{m}{mdiff} \quad \text{Eq. (1)}$$

where ρ = wood density (g.cm^{-3}); m = dry weight of the sample (g); and mdiff = weight difference of the submerged sample, which corresponds to its volume (cm^3). Subsequently, the wood samples were deposited in the xylotheque of the Herbarium of Museu Nacional (R).

The trees' AGB was determined to use allometry for tropical forest trees (Chave et al., 2014), substituting the values in Equation 2 for the obtained variables.

$$AGB = 0.063[\rho(DBH)^2 H)]^{0.976} \quad \text{Eq. (2)}$$

where, AGB = aboveground biomass (t.ha^{-1}), ρ = wood density (g.cm^{-3}), DBH = diameter at breast height (cm) and H = height (m). After the calculation, we used the AGB averages of the trees per plot as field information. Hereafter, this AGB calculated in field plots is treated as observed AGB (response variable).

Remote data

To estimate the AGB through modeling, we grouped the explanatory variables into five subsets that fall into two groups. The groups formed by individual data (from 1 to 4) and hybrid data (5) comprise the following subsets: (1) soil data, formed by eight soil variables from field collection; (2) spectral index data, formed by five indices calculated from remote sensing; (3) topographic attribute data, formed by seven variables derived from the digital elevation model (DEM); (4) environmental data, consisting of the selection of 15 bioclimatic variables acquired from the WorldClim 2.1 database (https://www.worldclim.org/data/index.html, accessed on: August 30, 2021); and (5) combined data, formed by the integration of all variables from the subsets mentioned above (35 variables). Below, we describe data collection and processing for the subsets, except for soil that was already described.

First, we acquired spectral index data from the United States Geological Survey (USGS) database (https://earthexplorer.usgs.gov/, accessed on August 31, 2021), an image taken by the Landsat 8 OLI/TIRS C1 L1 satellite with nine spectral bands. The product corresponds to point orbit 217-076, with a spatial resolution of 30 m, a temporal resolution of 16 days, minimum cloudiness, and an acquisition date of August 5, 2020 (the date is within the time range of the field collections). Then, we processed the spectral bands using the program QGIS 3.16.8 (QGIS, 2021) and the Semi-Automatic Classification Plugin 7.8.17 (SCP) (Congedo, 2016). We applied the dark object subtraction method (DOS) for atmospheric correction of the NIR, RED, BLUE, and GREEN bands. Subsequently, through the composition of bands and via the QGIS raster calculator (Graser et al., 2017), we estimated the five spectral indices (Table 1).

Table 1. Explanatory variables of spectral indices used in aboveground biomass (AGB) modeling in Serra da Tiririca. NIR (Near-Infrared) = Band 5; RED (Red) = Band 4; BLUE (Blue) = Band 2; GREEN (Green) = Band 3. Font: Zuñe et al. (2024).

Spectral indices	Name	Formula	Reference
NDVI	Normalized Difference Vegetation Index	$\frac{NIR - RED}{NIR + RED}$	Rouse et al. (1973)
SAVI	Soil Adjusted Vegetation Index	$(\frac{NIR - RED}{NIR + RED} + 0.5)(1.5)$	Huete (1988)
EVI	Enhanced Vegetation Index	$2.5(\frac{NIR - RED}{NIR + 6 * RED - 7.5 - BLUE + 1})$	Huete et al. (2002)
LAI	Leaf Area Index	$(18.37 * NDVI)$^1.51	Xavier &

			Vettorazzi (2004)
NDWI	Normalized Difference Water Index	$\frac{GREEN - NIR}{GREEN + NIR}$	Gao (1996)

Similarly, to obtain the topographic attribute data, we initially acquired a Shuttle Radar Topography Mission (SRTM) satellite image from the USGS database, corresponding to a DEM of 30 m spatial resolution, coordinates -23/-44, and a publication date of September 23, 2014. Then, we processed the image in QGIS, where we calculated all seven variables using a complement raster analysis (Table 2).

Table 2. Explanatory variables of topographic attributes used in the Serra da Tiririca AGB modeling. Font: Zuñe et al. (2024).

Variable	**Description**	**Reference**
Digital Elevation Model (DEM)	Altitude (m) of each plot	
Aspect (ASP)	Slop orientation concerning the north	Wilson & Gallant (2000)
Hillshade (HILLS)	The angle between the sun and the terrain surface	
Roughness Concentration Index (RCI)	Morphometric dissection patterns	Sampaio & Augustin (2014)
Slope (SLP)	The angle of inclination to the horizontal	
Topographic Position Index (TPI)	Compares the elevation of each cell to the elevation of a neighborhood	Guisan et al. (1999)
Terrain Ruggedness Index (TRI)	Express the amount of elevation difference between adjacent cells of a DEM	Riley et al. (1999)

To acquire the environmental data (Table 3), we accessed the WorldClim 2.1 database and selected the option bio30s (1 km^2 spatial resolution). We chose this option because it contains variables derived from average monthly values for temperature and precipitation over 1997–2000 (Fick et al., 2017).

Table 3. Explanatory variables of environmental data used in the Serra da Tiririca AGB modeling. Font: Zuñe et al. (2024).

Bioclimatic variables	**Description**
B1	Annual Mean Temperature
B2	Mean Diurnal Range [Mean of monthly (max temp - min temp)]
B3	Isothermality (B2/B7) ×100
B4	Temperature Seasonality (standard deviation ×100)
B5	Max Temperature of Warmest Month
B6	Min Temperature of Coldest Month
B7	Temperature Annual Range (B5-B6)
B8	Mean Temperature of Wettest Quarter
B9	Mean Temperature of Driest Quarter
B10	Mean Temperature of Warmest Quarter
B11	Mean Temperature of Coldest Quarter
B12	Annual Precipitation
B13	Precipitation of Wettest Month
B14	Precipitation of Driest Month
B15	Precipitation Seasonality (Coefficient of Variation)

All explanatory variables were in raster format, except the edaphic variables, whose values were found in the attribute tables of the coordinates of each plot in point shapefile format. Therefore, we converted the edaphic variables to raster by interpolating its values using the inverse distance weighting (IDW) deterministic method (Shepard, 1968), with the area's classification using SCP. To facilitate geoprocessing and data extraction, we cut all rasters from the dimensions of the base polygon (shapefile) of Serra da Tiririca. To extract the data values by plots of all

variables and redirect them to a single data array, we used QGIS's Point Sampling Tool 0.5.3 add-on.

Data analysis

First, to better understand this study, we described the results found in the field plots for the observed AGB and edaphic variables. Subsequently, using formulas described in Kersten & Galvão (2011), we verified the sampling sufficiency based on the number of individuals per plot, evaluating the sampling intensity and the optimal number of plots for the study area. Finally, we described the results of the relationships between field information and remote data, where we evaluated the performance of different modeling methods and selected the most suitable model to build an AGB map of the remnant.

We compared the accuracy of a semi-parametric method (generalized linear model, GLM) and a non-parametric method (random forest model, RF) to select the most accurate model. In recent years, both have been extensively explored in AGB modeling studies (e.g., Zhu & Liu, 2015; Lopatin et al., 2016; Almeida et al., 2019; Silveira et al., 2019; Schuh et al., 2020). For this reason, we decided to compare these two modeling approaches, making the following assumptions. First, GLM is a method that packs several statistical models into a single generalized model (Guisan et al., 2002) and, unlike other parametric modeling methods, uses data that does not assume a normal distribution and has a linking function for uniting the model components (McCullagh & Nelder, 2019). Second, RF is a set of learning methods based on deterministic techniques that integrate an extensive configuration of regression trees (Breiman, 2001). In turn, RF constantly selects random bootstrap samples from training data and has a final prediction of a weighted average of all regression trees (Cutler et al., 2012).

We randomly divided our data matrix into 60% training (6 sample plots) and 40% testing (4 sample plots) data to fit the models. This division was done with the createDataPartition function of the caret package 6.00-88 (Kuhn et al., 2016) in R 4.1.2 (R Core Team, 2021). Still, in R, we computed the two modeling methods using the MASS package (Ripley et al. 2013) and its functions to optimize the GLMs and the randomForest package (Liaw & Wiener, 2002) to adjust the parameters of the RF models.

Since GLMs work with parsimonious explanations (Guisan et al., 2002), we manually selected the best explanatory variables per subset for each model through the dropterm function. Considering all GLMs, we used the Gaussian distribution with the identity link. We submitted the explanatory variables to an analysis of variance with the F test to assess the goodness of fit of the models. We verified the measures of discrepancies through deviance residuals (Sakate et al., 2014). Finally, we selected the models with the lowest values according to the Akaike information criterion (AIC) (Burnham et al., 2011).

On the other hand, we used the percentage of explanation of the model variance (%var. explained) as a support metric for the RF model evaluation. We manually selected, for each model, the best explanatory variables based on the importance method (Liaw & Wiener, 2002). This method allowed us to calculate the mean decrease Gini (IncNodePurity) through the permutation out-of-bag data, which indicates the importance value of each variable for the model (Liaw & Wiener, 2002). Finally, we used 500 decision trees (ntree) for all models and left the random predictors per tree (mtry) as the default. Both modeling methods were trained by the training data and then applied to predict the AGB of the test data.

To assess the accuracy of the models, we related the observed AGB and the predicted AGB using simple linear regression. For this step, we measured the performance with the coefficient of determination (R^2), root means square error (RMSE, in $t.ha^{-1}$), and p-value <0.05, obtained through an analysis of variance (ANOVA). Subsequently, we selected the most accurate model (with the best performance). Through its prediction, we generated an AGB map of Serra da Tiririca in R using the functions of the raster package (Hijmans, 2021). We then imported the AGB map into QGIS to customize it. All maps in this study were generated from the Geographical Coordinate System and Datum WGS 84/UTM zone 23S (EPSG:32723).

Results

Aboveground biomass (AGB) and soil data

We registered 403 trees and observed, in the plots from 2019 to 2020, an AGB average of 371.12 ± 207.82 $t.ha^{-1}$ (range: 163.30 to 578.90 $t.ha^{-1}$) (Table 4). The granulometric composition of the soils had high percentages of sand and gravel, ranging from sandy soils with little gravel (Plots 2, 3, and 9) to sandy gravel soils (other plots) (Table 4). C, N, and P had the highest values in plots 9, 4, and 8, respectively (Table 4). The percentage of OM content was highest in plots 8 (8.39%) and 4 (6.60%) and lowest in plots

6 (3.48%) and 5 (44.0%) (Table 4). The sampling intensity was 0.45%, indicating the need to add 89 plots in the study area, based on the sampling sufficiency, to obtain stability in the number of individuals.

Table 4. Observed aboveground biomass (AGB) and soil data used in the Serra da Tiririca aboveground biomass modeling. ± = standard deviation; N = nitrogen; C = carbon; P = phosphorus; OM = organic matter. Font: Zuñe et al. (2024).

Plots (Number of trees)	AGB observed	Edaphic variables							
		Gravel	Sand	Silt	Clay	N	C	P	OM
	($t.ha^{-1}$)	(%)					($mg.g^{-1}$)		(%)
1 (32)	746.50 ± 909.24	18.47	72.76	8.35	0.42	1.82	20.62	0.20	5.13
2 (35)	280.19 ± 301.43	9.02	84.56	5.63	0.79	1.82	13.67	0.13	4.49
3 (33)	662.03 ± 670.22	8.62	83.73	7.08	0.58	2.43	23.68	0.15	6.25
4 (26)	627.18 ± 1122.21	25.82	72.28	1.86	0.04	3.08	31.87	0.12	6.60
5 (40)	149.37 ± 111.67	23.60	72.40	3.79	0.21	1.40	17.20	0.07	4.10
6 (49)	203.17 ± 268.35	22.85	68.75	7.70	0.70	1.42	18.09	0.02	3.48
7 (92)	255.19 ± 437.39	26.00	70.30	3.51	0.19	1.47	17.64	0.10	4.54
8 (32)	324.87 ± 461.52	20.43	73.73	5.54	0.30	2.02	28.34	0.22	8.39
9 (31)	247.05 ± 207.02	13.50	80.33	6.03	0.14	2.27	32.86	0.05	5.96
10 (33)	215.61 ± 161.25	23.35	70.96	5.34	0.35	1.45	20.01	0.02	4.64
Average	**371.12 ± 207.82**	**19.17 ± 5.95**	**74.98 ± 5.42**	**5.48 ± 1.89**	**0.37 ± 0.23**	**1.92 ± 0.51**	**22.40 ± 6.23**	**0.11 ± 0.06**	**5.35 ± 1.37**

Comparison between GLM and RF approaches

The random partition selected plots 2, 3, 4, 6, 7, and 10 for the training data and plots 1, 5, 8, and 9 for the test data. For the construction of the GLMs, the variables that best explained the observed AGB variation were the following: Silt, P, and C for the soil data subset; SAVI, NDVI, and LAI for the spectral index data subset; DEM, SLP, and TPI for the topographic attribute data subset; B1, B9, and B12 for the environmental data subset; and B4, SLP, SAVI, and N for the combined data subset (Table 5). For the construction of the RF models, all variables of each subset were used, notably the essential variables for the model explanations: OM, C, and N for the soil data subset; NDVI, SAVI, and NDWI for the spectral index data subset; TPI, DEM, and HILLS for the topographic attribute data subset; B3, B13, and B6 for the environmental data subset; and N, TPI, B3, and EVI for the combined data subset (Table 5). The evaluation of the deviance residuals of the GLMs showed that the selection of variables from the saturated model contributed to a better explanation of the models, with low AIC values and significance for the variables selected by the subset (Table 5). The explained variance of the RF models had negative values for the topographic attribute and spectral index subsets, while the other subsets had low positive values (Table 5).

Table 5. Models with training data using a general linear model (GLM) and random forest (RF) model for observed aboveground biomass (AGB) effects on subsets. GLMs show the coefficients of the variables selected by the subgroup to build the models. In contrast, the RF models show the most important variables of the models in each subset. Positive parameters in GLMs indicate positive effects, and negative parameters indicate negative effects. p>(F) = 0.001 '***', 0.01 '**', 0.5 '*', 0.1 '.'; ns = not significant. Font: Zuñe et al. (2024).

GLM training results			RF training results	
***Subset* / variables**	**Estimate (Std. error)**	**Res. Deviance (AIC)**	***Subset* / variables**	**% var. explained / IncNodePurity (%)**
Soils	-574.18 (58.05)	224248 (57.05)	*Soils*	*18.53*
Silt	33.01 (5.15) *	209599	OM	98.65
P	2300.33 (175.29) **	108005	C	79.94
C	27.36 (1.77) **	895	N	73.01
Spectral indices	53534.50 (13054.50)	224248 (74.05)	*Spectral indices*	*-95.31*
SAVI	-6853.80 (1327.30) ns	210061	NDVI	98.52
NDVI	-224812.40 (54673.10) ns	145706	SAVI	95.82
LAI	2239.90 (538.70) .	15109	NDWI	90.96
Topographic attributes	366.85 (34.45)	224248 (62.10)	*Topographic attributes*	*-27.98*
DEM	-2.41 (0.37) *	174781	TPI	94.28
SLP	25.37 (3.17) ***	28414	DEM	44.01
TPI	-84.23 (16.77) *	2075	HILLS	42.92
Environmental	874.89 (7568.54)	224248 (73.35)	*Environmental*	*11.73*
B1	-8456.37 (1818.47) ns	204952	B3	94.58
B9	8510.30 (1618.99) *	53946	B13	85.84
B12	16.70 (6.83) ns	13529	B6	80.58

Combined	297.18 (16.43)	224248 (1.39)	*Combined*	*2.71*
B4	-5.96 (0.07) ***	145440	N	98.64
SLP	6.07 (0.38) ***	114119	TPI	94.25
SAVI	1251.03 (2.45) **	100454	B3	72.79
N	361.84 (0.27) ***	0	EVI	10.68

When testing the GLM and RF models, there were large differences in the performance of each subset (Figure 2). The performance of the GLMs showed a 67% reduction in the RMSE of the individual data subsets compared to the combined subset (from 288.53 to 94.36 $t.ha^{-1}$), while in the RF models, for the same comparison, there was a 30% decrease (from 98.76 to 68.17 $t.ha^{-1}$) (Figure 2). When comparing individual GLM and RF data subsets, RF performed better for the spectral index, topographic attribute, and environmental data subsets. In contrast, GLM performed better only for the soil data subset (Figure 2a-h). When comparing the subset of combined data, the GLM had greater explanatory potential (R^2 = 0.65) than the RF (R^2 = 0.57). However, RF had a lower RMSE (68.17 $t.ha^{-1}$) than the GLM (94.36 $t.ha^{-1}$). Both were significant (Figure 2i-j). Among all models, the best-performing model was from the topographic attribute data subset of the RF modeling method (R^2 = 0.82, RMSE = 32.14 $t.ha^{-1}$, p = 0.0002) (Figure 2f).

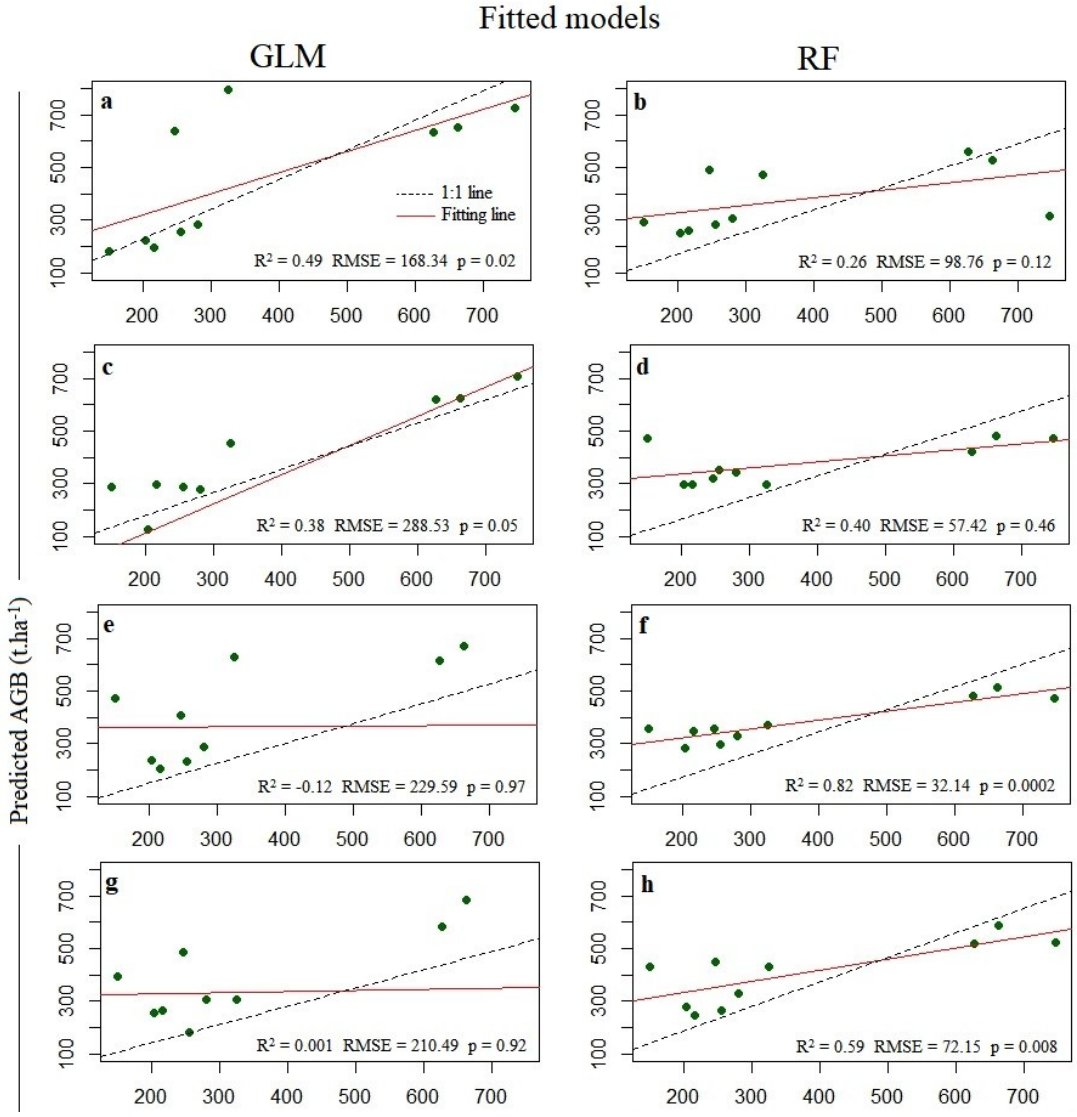

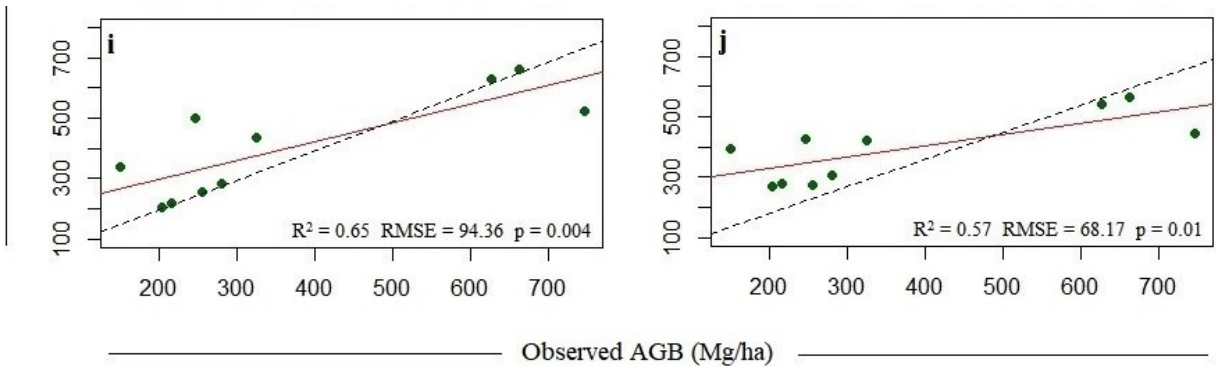

Figure 2. Observed aboveground biomass (AGB) *versus* predicted AGB using the general linear model (GLM) and random forest (RF) methods with the following as input: a-b, soil data; c-d, spectral indices; e-f, topographic attributes; g-h, environmental data; and i-j, the combination of all data. RMSE = root mean square error. Dotted lines = identity line. Full red lines = fitting line. Font: Zuñe et al. (2024).

Constructing the aboveground biomass (AGB) map

To construct the Serra da Tiririca AGB map, we chose the GLM model of the combined subset, which is the most accurate compared to the RF for our remnant. This model estimated an average AGB of 405.31 ± 160.79 t.ha^{-1}. The current estimation of AGB in the study area showed areas with low AGB values in the north and south terminals and places close to rock formations. In contrast, the remnant's interior had intermediate and high AGB values (Figure 3).

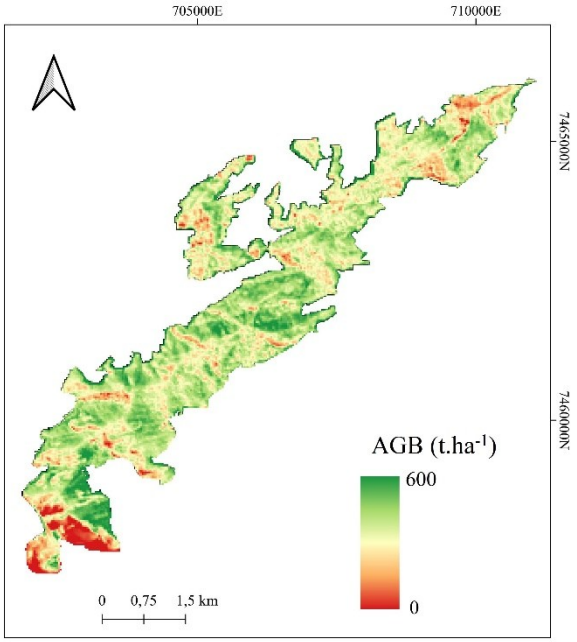

Figure 3. Aboveground biomass (AGB) estimation map of Serra da Tiririca between 2019 and 2020, applying the GLM modeling method using combined soil, spectral index, topographic attribute, and environmental data. Font: Zuñe et al. (2024).

Discussion

Improving AGB and soil data estimates is essential to understand spatial distribution patterns in tropical forests (Chave et al., 2019). This study aimed to determine the AGB of an Atlantic Forest remnant and select the most accurate modeling method to generate an AGB map of the area. We also evaluated the best approach (GLM or RF) to generate the map. We found an AGB average of 371 t.ha^{-1} and selected the combined data of the GLM method to create the map. Combining soil variables, remote sensing, and environmental data improved the GLM and RF models.

In tropical forests, AGB spatial distribution patterns are very dynamic (Poorter et al., 2016). For example, a range between 50 and 300 t.ha^{-1} is widely reported for the Atlantic Forest (e.g., Cunha et al., 2009; Alves et al., 2010; Medeiros & Aidar, 2011; Silva et al., 2018; Silveira et al., 2019). However, few studies report values above this range (e.g., Rolim et al., 2005; Lindner & Sattler, 2012). Here, we predict an AGB average of 405 t.ha^{-1}, which would easily fit within the reported range for Amazonian rainforest (between 100 and 500 t.ha^{-1}) (Nascimento et al., 2002; Saatchi et al., 2002; Saatchi et al., 2007; Mazzei et al., 2010; Benítez et al., 2016). Our prediction could be primarily influenced by the type of vegetation in the remnant. Serra da Tiririca is a heterogeneous forest at different successional stages and has a high diversity of trees (Barros, 2008; Zuñe-da-Silva et al., 2023). Therefore, when not treated as outliers, a few large trees in areas with a high density of small trees would directly influence the variability of the means and standard deviation of AGB in the field plots.

Among other factors that could have influenced our AGB prediction, such as plot size and sample size (Chave et al., 2004), explanatory variables play an essential role (Silveira et al.,

2019). Soil properties, for example, are necessary to understand the variability in structure, such as AGB (Poorter et al., 2015). This study found a soil pattern like other Atlantic Forest remnants (Sanchez et al., 2013; Diniz et al., 2015; Cysneiros et al., 2021). However, unlike the other edaphic variables, we observed that organic carbon (C), nitrogen (N), and phosphorus (P) contributed the most to explaining the variation in AGB in the models, both with individual and combined data. This contribution could be explained by the positive correlation between these elements (C, N, and P) and AGB stocks in tropical forests (Laurance et al., 1999). However, in the Atlantic Forest, mainly in coastal remnants, it has been observed that the variation in AGB related to the concentration of these elements could be affected by climatological and topographic variables (Alves et al., 2010; Vieira et al., 2011; Martins et al., 2015). Other edaphic variables in this study had little influence on the models, such as particle size and organic matter. Although, depending on the type of Atlantic Forest vegetation, they could be a good predictor of AGB (Toledo et al., 2018).

Other predictor variables derived from remote sensing, such as spectral indices, have often shown a strong relationship with AGB predictions (Gasparri et al., 2010; Ferraz et al., 2014; Zhu & Liu, 2015). However, depending on the vegetation density, some indices might not be appropriate for predicting AGB (Lu et al., 2016). Here, the spectral indices did not act as good predictors of AGB. However, we observed that SAVI was the most significant explanatory potential variable. It was important in explaining the individual data models and was significant to justify the most suitable model to generate the Serra da Tiririca AGB map. SAVI corrects the NDVI in remote sensing by applying the ground brightness correction factor (Huete, 1988). Although the SAVI is often better at predicting the AGB of agricultural areas (Ren et al., 2018), it also correlates highly with the AGB of tropical rainforests (Debastini et al., 2019).

Similar to spectral indices, topographic attributes have great potential to predict AGB (Asner et al., 2009). This study found that the DEM, TPI, and SLP variables contributed the most to explaining the models with individual and hybrid data. For the Atlantic Forest, a positive relationship has been observed between these topographic attributes and AGB. AGB increases as the altitude increases (Alves et al., 2010). On the other hand, using topographic attributes derived from remote sensing in AGB predictions could be a key part of estimating AGB in the Atlantic Forest because adding these attributes would significantly improve the models' predictions (Barbosa et al., 2014).

Among the numerous abiotic variables that predict ecological processes, climatological variables are the most explored (Fick et al., 2017). Here, we found that the distinct bioclimatic variables associated with temperature were essential to explaining the variation of AGB in models with individual and hybrid data. However, for the Atlantic Forest, bioclimatic variables explain only a small portion of the AGB models (David et al., 2017). Nevertheless, just as the individual variables were essential to explaining the different models, combining these variables significantly improved the explanations of the hybrid models. As shown in other studies of Atlantic Forest (e.g., Silveira et al., 2019), the combination of these predictive variables increased the performance of the AGB predictive models.

The accuracy of AGB predictions can vary significantly between different modeling methods (Zhu & Liu, 2015). Here, we found that RF models, with both individual and hybrid data, had low RMSE compared to GLMs. On the other hand, the GLMs had a higher R^2 than the RF models. Although both methods have efficient models, a GLM is more accurate for AGB estimates than an RF in sclerophyllous forests (Lopatin et al., 2016) and tropical rainforests (Schuh et al., 2020). We also observed that the selection of variables is essential for explaining the models, especially in the RF models, where we had negative values for the percentage of the variance of the models with the topographic attribute and spectral indices variables. These negative values could indicate that the model is poorly supported, resulting in a very weak or erroneous performance (Breiman, 2001). Finally, we generated the AGB map of Serra da Tiririca using the GLM with combined data because it had greater explanatory potential than the RF model with combined data. Additionally, although the RF model with combined data has a lower RMSE than the GLM with combined data, the latter showed a higher percentage of RMSE reduction than models with individual data.

Although accurately estimating the AGB of large areas is still challenging, in this study, we observed that comparing modeling methods and predictor variables results in a better model for estimating AGB in an Atlantic Forest remnant. This is the first study that estimates AGB for PESET. The AGB map generated in this study enables us to understand the spatial distribution patterns of AGB in Serra da Tiririca. In addition,

it will contribute to implementing better management practices in the study area. Finally, it is essential to evaluate other coastal remnants following this same line of research to improve the AGB estimates and better understand Atlantic Forest AGB patterns.

Conclusion

We estimated an AGB of 371.12 ± 207.82 t.ha^{-1} in field plots of Serra da Tirrica. For Serra da Tiririca, the comparison between modeling methods showed that a GLM is more accurate, but an RF model is also fit to estimate the AGB. This more accurate modeling method predicted an AGB of 405.31 t.ha^{-1}. Additionally, we found that the performance of the models improved when we combined predictor variables from the soil, remote sensing, and environmental data. The AGB map generated from the GLM with combined data showed that the highest AGB stocks are concentrated in the interior of the remnant. Finally, the AGB map of the protected area will contribute to implementing management and prevention action.

Acknowledgments

We want to thank the Coordenação de Aperfeiçoamento de Pessoal de Nível Superior (CAPES) for granting the master's scholarship to the first author. The authors give a special thanks to the Serra da Tiririca State Park (PESET) coordinator, André Costa, and the park rangers, Erbersson da Conceição, Rafael Fonseca, and Ângelo Coutinho, for the field support.

References

Ali, A.; Lin, S. L.; He, J. K.; Kong, F. M.; Yu, J. H.; Jiang, H. S. 2019. Elucidating space, climate, edaphic, and biodiversity effects on aboveground biomass in tropical forests. Land Degradation & Development, 30, (8), 918-927. https://doi.org/10.1002/ldr.3278

Almeida, C. T.; Galvao, L. S.; Ometto, J. P. H. B.; Jacon, A. D.; Pereira, F. R. S.; Sato, L. Y.; Lopes, A. P.; Graça, P. M. L. A.; Silva, C. V. J.; Ferreira-Ferreira, J.; Longo, M. 2019. Combining LiDAR and hyperspectral data for aboveground biomass modeling in the Brazilian Amazon using different regression algorithms. Remote Sensing of Environment, 232, (2019), 111323. https://doi.org/10.1016/j.rse.2019.111323

Alvares, C. A.; Stape, J. L.; Sentelhas, P. C.; Gonçalves, J. L. M.; Sparovek, G. 2013. Köppen's climate classification map for Brazil. Meteorologische Zeitschrift, 2, (6), 711-728. https://doi.org/10.1127/0941-2948/2013/0507

Alves, L. F.; Vieira, A. S.; Scaranello, M. A.; Camargo, P. B.; Santos, F. A.; Joly, C. A.; Martinelli, L. A. 2010. Forest structure and live aboveground biomass variation along an elevational gradient of tropical Atlantic moist forest (Brazil). Forest ecology and management, 260, (5), 679-691. https://doi.org/10.1016/j.foreco.2010.05.023

Asner, G. P.; Hughes, R. F.; Varga, T. A; Knapp, D. E.; Kennedy-Bowdoin, T. 2009. Environmental and biotic controls over aboveground biomass throughout a tropical rain forest. Ecosystems, 12, (2), 261-278. https://doi.org/10.1007/s10021-008-9221-5

ABNT. Associação Brasileira de Normas Técnicas. 2003. Madeira: determinação da densidade básica: NBR 11941. Rio de Janeiro. 6p.

Avitabile, V.; Herold, M.; Heuvelink, G. B.; Lewis, S. L.; Phillips, O. L.; Asner, G. P.; Armston, J.; Ashton, P. S.; Banin, L.; Bayol, N.; Berry, N. J.; Boeckx, P.; Jong, B. H. J.; DeVries, B.; Girardin, C. A. J.; Kearsley, E.; Lindsell, J. A.; Lopez-Gonzalez, G.; Lucas, R.; Malhi, Y.; Morel, A.; Mitchard, E. T. A.; Nagy, L.; Qie, L. Quinones, M. J.; Ryan, C. M.; Slik, J. W.; Sunderland, T. F.; Laurin, G. V.; Gatti, R. C.; Valentini, R.; Verbeeck, H.; Wijaya, A.; Willcock, S. 2016. An integrated pan-tropical biomass map using multiple reference datasets. Global change biology, 22, (4), 1406-1420. https://doi.org/10.1111/gcb.13139

Barbosa, J. M.; Melendez-Pastor, I.; Navarro-Pedreño, J.; Bitencourt, M. D. 2014. Remotely sensed biomass over steep slopes: An evaluation among successional stands of the Atlantic Forest Brazil. ISPRS Journal of Photogrammetry and Remote Sensing, 88, (2014), 91-100. https://doi.org/10.1016/j.isprsjprs.2013.11.019

Barros, A. A. M. 2008. Análise florística e estrutural do Parque Estadual da Serra da Tiririca, Niterói e Maricá, RJ, Brasil. Tese de Doutorado. Escola Nacional de Botânica Tropical, Instituto de Pesquisas Jardim Botânico do Rio de Janeiro, Rio de Janeiro, Brasil. 225p.

Benitez, F. L.; Anderson, L. O.; Formaggio, A. R. 2016. Evaluation of geostatistical techniques to estimate the spatial distribution of aboveground biomass in the Amazon rainforest using high-resolution remote sensing data. Acta Amazonica, 46, (2), 151-

160. https://doi.org/10.1590/1809-4392201501254

Breiman, L. 2001. Random forests. Machine learning, 45, (1), 5-32.

Burnham, K. P.; Anderson, D. R.; Huyvaert, K. P. 2011. AIC model selection and multimodel inference in behavioral ecology: some background, observations, and comparisons. Behavioral ecology and sociobiology, 65, (1), 23-35. https://doi.org/10.1007/s00265-010-1029-6

Chave, J.; Condit, R.; Aguilar, S.; Hernandez, A.; Lao, S.; Perez, R. 2004. Error propagation and scaling for tropical forest biomass estimates. Philosophical Transactions of the Royal Society of London. Series B: Biological Sciences, 359, (1443), 409-420. https://doi.org/10.1098/rstb.2003.1425

Chave, J. 2006. Measuring wood density for tropical forest trees: A field manual, Pan-Amazonia Project. 6p.

Chave, J.; Réjou-Méchain, M.; Búrquez, A.; Chidumayo, E.; Colgan, M. S.; Delitti, W. B. C; Duque, A.; Eid, T.; Fearnside, P. M.; Goodman, R. C.; Henry, M.; Martínez-Yrízar, A.; Mugasha, W. A.; Muller-Landau, H. C.; Mencuccini, M.; Nelson, B. W.; Ngomanda, A.; Nogueira, E. M.; Ortiz-Malavassi, E.; Pélissier, R.; Ploton, P.; Ryan, C. M.; Saldarriaga, J. G.; Vieilledent, G. 2014. Improved allometric models to estimate the aboveground biomass of tropical trees. Global change biology, 20, (10), 3177-3190. https://doi.org/10.1111/gcb.12629

Chave, J.; Davies, S. J.; Phillips, O. L.; Lewis, S. L..; Sist, P.; Schepaschenko, D.; Armston, J.; Baker, T. R.; Coomes, D.; Disney, M.; Duncanson, L.; Hérault, B.; Labrière, N.; Meyer, V.; Réjou-Méchain, M.; Scipal, K.; Saatchi, S. 2019. Ground data are essential for biomass remote sensing missions. Surveys in Geophysics, 40, (4), 63-880. https://doi.org/10.1007/s10712-019-09528-w

Chazdon, R. L. 2003. Tropical forest recovery: legacies of human impact and natural disturbances. Perspectives in Plant Ecology, evolution and systematics, 6, (1-2), 51-71. https://doi.org/10.1078/1433-8319-00042

Congedo, L. 2016. Semi-automatic classification plugin documentation. Release, 4, (0.1), 29.

Cunha, G. D. M; Gama-Rodrigues, A. C.; Gama-Rodrigues, E. F.; Velloso, A. C. X. 2009. Biomassa e estoque de carbono e nutrientes em florestas montanas da Mata Atlântica na região norte do estado do Rio de Janeiro. Revista Brasileira de Ciência do Solo, 33, (5), 1175-1185. https://doi.org/10.1590/S0100-06832009000500011

Cutler, A.; Cutler, D. R.; Stevens, J. R. 2012. Random forests. In: Ensemble machine learning. Springer, Boston, MA. pp. 157-175.

Cysneiros, V. C.; Souza, F. C.; Gaui, T. D.; Pelissari, A. L.; Orso, G. A.; Machado, S. A.; Silveira-Filho, T. B. 2021. Integrating climate, soil and stand structure into allometric models: An approach of site-effects on tree allometry in Atlantic Forest. Ecological Indicators, 127, (2021), 107794. https://doi.org/10.1016/j.ecolind.2021.107794

David, H. C.; Araújo, E. J. G.; Morais, V. A.; Scolforo, J. R. S.; Marques, J. M.; Netto, S. P.; MacFarlane, D. W. 2017. Carbon stock classification for tropical forests in Brazil: Understanding the effect of stand and climate variables. Forest Ecology and Management, 404, (2017), 241-250. https://doi.org/10.1016/j.foreco.2017.08.044

Debastiani, A. B.; Moura, M. M.; Rex, F. E.; Sanquetta, C. R.; Corte, A. P. D.; Pinto, N. 2019. Regressões robusta e linear para estimativa de biomassa via imagem sentinel em uma floresta tropical. BIOFIX Scientific Journal, 4, (2), 81-87. https://doi.org/10.5380/biofix.v4i2.62922

Diniz, A. R.; Machado, D. L.; Pereira, M. G.; Balieiro, F. D. C.; Menezes, C. E. G. 2015. Biomassa, estoques de carbono e de nutrientes em estádios sucessionais da Floresta Atlântica, RJ. Embrapa Solos-Artigo em periódico indexado, 11p.

EMBRAPA. Empresa Brasileira de Agropecuária. 1997. Manual de métodos de análise de solo. Embrapa Solos, Rio de Janeiro. 212p.

EMBRAPA. Empresa Brasileira de Agropecuária. 2018. Sistema brasileiro de classificação de solos. 5a ed. Embrapa, Brasília. 353p.

Ferraz, A. S.; Soares, V. P.; Soares, C. P. B.; Ribeiro, C. A. A. S.; Binoti, D. H. B.; Leite, H. G. 2014. Estimativa do estoque de biomassa em um fragmento florestal usando imagens orbitais. Floresta e Ambiente, 21, (3), 286-296. https://doi.org/10.1590/2179-8087.052213

Fick, S. E.; Hijmans, R. J. 2017. WorldClim 2: new 1km spatial resolution climate surfaces for global land areas. International Journal of Climatology, 37, (12), 4302-4315. https://doi.org/10.1002/joc.5086

Gao, B. C. 1996. NDWI-A normalized difference water index for remote sensing of vegetation

liquid water from space. Remote sensing of environment, 58, (3), 257-266. https://doi.org/10.1016/S0034-4257(96)00067-3

Gagliasso, D.; Hummel, S.; Temesgen, H. 2014. A comparison of selected parametric and non-parametric imputation methods for estimating forest biomass and basal area. Open Journal of Forestry, 4, (1), 42-48. https://doi.org/10.4236/ojf.2014.41008

Gasparri, N. I.; Parmuchi, M. G.; Bono, J.; Karszenbaum, H.; Montenegro, C. L. 2010. Assessing multi-temporal Landsat 7 ETM+ images for estimating aboveground biomass in subtropical dry forests of Argentina. Journal of Arid Environments, 74, (10), 1262-1270. https://doi.org/10.1016/j.jaridenv.2010.04.007

Goward S.; Arvidson T.; Williams D.; Faundeen J.; Irons J.; Franks S. 2006. Historical record of Landsat global coverage. Photogrammetric Engineering & Remote Sensing, 72, (10), 1155-1169. https://doi.org/10.14358/PERS.72.10.1155

Graser, A.; Mearns, B.; Mandel, A.; Ferrero, V. O.; Bruy, A. 2017. QGIS: Becoming a GIS power user. Packt Publishing Ltd. 818p

Guisan, A.; Weiss, S. B.; Weiss, A. D. 1999. GLM versus CCA Spatial Modeling of Plant Species Distribution. Plant Ecology, 143, (1999), 107-122. https://doi.org/10.1023/A:1009841519580

Guisan, A.; Edwards Jr, T. C.; Hastie, T. 2002. Generalized linear and generalized additive models in studies of species distributions: setting the scene. Ecological modelling, 157, (2-3), 89-100. https://doi.org/10.1016/S0304-3800(02)00204-1

Hansen, M. C.; Potapov, P. V.; Moore, R.; Hancher, M.; Turubanova, S. A.; Tyukavina, A.; Thau, D.; Stehman, S. V.; Goetz, S. J.; Loveland, T. R.; Kommareddy, A.; Egorov, A.; Chini, L.; Justice, C. O.; Townshend, J. R. G. 2013. High-resolution global maps of 21st-century forest cover change. Science, 342, (6160), 850-853. https://doi.org/10.1126/science.12446

Hijmans, R. J. 2021. Geographic Data Analysis and Modeling [R package raster version 3.4-10].

Huete, A. A. 1998. Soil-adjusted vegetation index (SAVI). Remote Sensing of Environment. Remote sensing of environment, 25, (1998), 295-309.

Huete, A.; Didan, K.; Miura, T.; Rodriguez, E. P.; Gao, X.; Ferreira, L. G. 2002. Overview of the radiometric and biophysical performance of the MODIS vegetation indices. Remote sensing of environment, 83, (1-2), 195-213. https://doi.org/10.1016/S0034-4257(02)00096-2

Houghton, R. A. 2005. Aboveground Forest biomass and the global carbon balance. Global change biology, 11, (6), 945-958. https://doi.org/10.1111/j.1365-2486.2005.00955.x

INEA. Instituto Estadual do Ambiente. 2015. Plano de Manejo do Parque Estadual da Serra da Tiririca. Governo do Estado do Rio de Janeiro. 105p.

Kersten, R. A.; Galvão F. 2011. Suficiência amostral em inventários florísticos e fitossociológicos. In: Felfili, J. M. et al. Fitossociologia no Brasil: métodos e estudos de casos. Editora UFV. Viçosa, MG. pp. 156-173.

Kuhn, M.; Wing, J.; Weston, S.; Williams, A.; Keefer, C.; Engelhardt, A.; Cooper, T. 2016. Caret: Classification and Regression Training (version 6.0-64).

Laurance, W. F.; Fearnside, P. M.; Laurance, S. G.; Delamonica, P.; Lovejoy, T. E.; Merona, J. M. R.; Chambers, J. Q.; Gascon, C. 1999. Relationship between soils and Amazon forest biomass: a landscape-scale study. Forest Ecology and Management, 118, (1-3), 127-138. https://doi.org/10.1016/S0378-1127(98)00494-0

Laurance, W. F.; Camargo, J. L.; Fearnside, P. M.; Lovejoy, T. E.; Williamson, G. B.; Mesquit, R. C.; Meyer, C. F. J.; Bobrowiec, P. E. D.; Laurance, S. G. W. 2018. An Amazonian rainforest and its fragments as a laboratory of global change. Biological Reviews, 93, (1), 223-247. https://doi.org/10.1111/brv.12343

Li, Y.; Li, C.; Li, M.; Liu, Z. 2019. Influence of variable selection and forest type on forest aboveground biomass estimation using machine learning algorithms. Forests, 10, (12), 1073. https://doi.org/10.3390/f10121073

Liaw, A.; Wiener, M. 2002. Classification and regression by randomForest. R news, 2, (3), 18-22.

Lindner, A.; Sattler, D. 2012. Biomass estimations in forests of different disturbance history in the Atlantic Forest of Rio de Janeiro, Brazil. New Forests, 43, (3), 287-301. https://doi.org/10.1007/s11056-011-9281-9

Lopatin, J.; Dolos, K.; Hernández, H. J.; Galleguillos, M.; Fassnacht, F. E. 2016. Comparing generalized linear models and random forest to model vascular plant species richness using LiDAR data in a natural forest in central Chile. Remote Sensing of Environment, 173, (2016), 200-210. https://doi.org/10.1016/j.rse.2015.11.029

Lu, D.; Mausel, P.; Brondızio, E.; Moran, E. 2004. Relationships between forest stand parameters and Landsat TM spectral responses in the Brazilian Amazon Basin. Forest Ecology and Management, 198, (1-3), 149-167. https://doi.org/10.1016/j.foreco.2004.03.048

Lu, D. 2005. Aboveground biomass estimation using Landsat TM data in the Brazilian Amazon. International Journal of Remote Sensing, 26, (12), 2509-2525. https://doi.org/10.1080/01431160500142145

Lu, D.; Chen, Q.; Wang, G.; Liu, L.; Li, G.; Moran E. 2016. A survey of remote sensing-based aboveground biomass estimation methods in forest ecosystems. International Journal of Digital Earth, 9, (1), 63-105. https://doi.org/10.1080/17538947.2014.990526

Nascimento, H. E. M.; Laurance, W. F.; 2002. Total aboveground biomass in central Amazonian rainforests: a landscape-scale study. Forest Ecology and Management, 168, (1-3), 311-321. https://doi.org/10.1016/S0378-1127(01)00749-6

Martins, S. C.; Sousa Neto, E.; Piccolo, M. C.; Almeida, D.; Camargo, P.; Carmo, J. B.; Porder, S.; Lins, R. S. M.; Martinelli, L. A. 2015. Soil texture and chemical characteristics along an elevation range in the coastal Atlantic Forest of Southeast Brazil. Geoderma Regional, 5, (2015), 106-116. https://doi.org/10.1016/j.geodrs.2015.04.005

Mazzei, L.; Sist, P.; Ruschel, A.; Putz, F. E.; Marco, P.; Pena, W.; Ferreira, J. E. R. 2010. Aboveground biomass dynamics after reduced-impact logging in the Eastern Amazon. Forest Ecology and Management, 259, (3), 367-373. https://doi.org/10.1016/j.foreco.2009.10.031

McCullagh, P.; Nelder, J. A. 2019. Generalized linear models. Routledge. 532p. https://doi.org/10.1201/9780203753736

Medeiros, M. C. M. P. D.; Aidar, M. P. M. 2011. Structural variation and content of aboveground living biomass in an area of Atlantic Forest in the State of São Paulo, Brazil. Hoehnea, 38, (3), 413-428. https://doi.org/10.1590/S2236-89062011000300004

Meira Junior, M. S.; Pinto, J. R. R.; Ramos, N. O.; Miguel, E. P.; Gaspar, R. D. O.; Phillips, O. L. 2020. The impact of long dry periods on the aboveground biomass in a tropical forest: 20 years of monitoring. Carbon balance and management, 15, (12), 1-14. https://doi.org/10.1186/s13021-020-00147-2

Mitchard, E. T. A. 2018. The tropical forest carbon cycle and climate change. Nature, 559, (7715), 527-534. https://doi.org/10.1038/s41586-018-0300-2

Myers, N.; Mittermeier, R. A.; Mittermeier, C. G.; Fonseca, G. A.; Kent, J. 2000. Biodiversity hotspots for conservation priorities. Nature, 403, (6772), 853-858. https://doi.org/10.1038/35002501

Pan, Y.; Birdsey, R. A.; Fang, J.; Houghton, R.; Kauppi, P. E.; Kurz, W. A.; Phillips, O. L.; Shvidenko, A.; Lewis, S. L.; Canadell, J. G.; Ciais, P.; Jackson, R. B.; Pacala, S. W.; McGuire, A. D.; Piao, S.; Rautiainen, A.; Sitch, S.; Hayes, D. 2011. A large and persistent carbon sink in the world's forests. Science, 333, (6045), 988-993. https://doi.org/10.1126/science.1201609

Poorter, L.; van der Sande, M. T.; Thompson, J.; Arets, E. J.; Alarcón, A.; Álvarez-Sánchez, J.; Ascarrunz, N.; Balvanera, P.; Barajas-Guzmán, G.; Boit, A.; Bongers, F.; Carvalho, F. A.; Casanoves, F.; Cornejo-Tenorio, G.; Costa, F. R. C.; Castilho, C. V.; Duivenvoorden, J. F.; Dutrieux, L. P.; Enquist, B. J.; Fernández-Méndez, F.; Finegan, B.; Gormley, L. H. L.; Healey, J. R.; Hoosbeek, M. R.; Ibarra-Manríquez, G.; Junqueira, A. B.; Levis, C.; Licona, J. C.; Lisboa, L. S.; Magnusson, W. E.; Martínez-Ramos, M.; Martínez-Yrizar, A.; Martorano, L. G.; Maskell, L. C.; Mazzei, L.; Meave, J. A.; Mora, F.; Muñoz, R.; Nytch, C.; Pansonato, M. P.; Parr, T. W.; Paz, H.; Pérez-García, E. A.; Rentería, L. Y.; Rodríguez-Velazquez, J.; Rozendaal, D. M. A.; Ruschel, A. R.; Sakschewski, B.; Salgado-Negret, B.; Schietti, J.; Simões, M.; Sinclair, F. L.; Souza, P. F.; Souza, F. C.; Stropp, J.; Steege, H.; Swenson, N. G.; Thonicke, K.; Toledo, M.; Uriarte, M.; van der Hout, P.; Walker, P.; Zamora, N.; Peña-Claros, M. 2015. Diversity enhances carbon storage in tropical forests. Global Ecology and Biogeography, 24, (11), 1314-1328. https://doi.org/10.1111/geb.12364

Poorter, L.; Bongers, F.; Aide, T.M.; Zambrano, A. M. A.; Balvanera, P.; Becknell, J. M.; Boukili, V.; Brancalion, P. H. S.; Broadbent, E. N.; Chazdon, R. L.; Craven, D.; Almeida-Cortez, J. S.; Cabral, G. A. L.; Jong, B. H. J.; Denslow, J. S.; Dent, D. H.; DeWalt, S. J.; Dupuy, J. M; Durán, S. M.; Espírito-Santo, M. M.; Fandino, M. C.; César, R. G.; Hall, J. S.; Hernandez-Stefanoni, J. L.; Jakovac, C. C.; Junqueira, A. B.; Kennard, D.; Letcher, S. G.; Licona, J. C.; Lohbeck, M.; Marín-Spiotta, E.; Martínez-Ramos, M.; Massoca, P.; Meave, J. A.; Mesquita, R.; Mora, F.; Muñoz, R.; Muscarella, R.; Nunes, Y. R. F.; Ochoa-Gaona, S.; Oliveira, A. A.; Orihuela-Belmonte, E.; Peña-Claros, M.; Pérez-García, E. A.; Piotto, D.; Powers, J. S.; Rodríguez-Velázquez, J.; Romero-Pérez, I. E.; Ruíz, J.; Saldarriaga, J.G.; Sanchez-Azofeifa, A.; Schwartz, N. B.; Steininger, M. K.; Swenson, N. G.; Toledo, M.; Uriarte, M.; van Breugel, M.; van der Wal, H.; Veloso, M. D. M.; Vester, H. F. M.; Vicentini, A.; Vieira, I. C .G.; Vizcarra Bentos, T.; Williamson, G. B.; Rozendaal, D. M. A. 2016. Biomass resilience of Neotropical secondary forests. Nature, 530, (7589), 211-214. https://doi.org/10.1038/nature16512

Poorter, L.; van der Sande, M. T.; Arets, E. J.; Ascarrunz, N.; Enquist, B. J.; Finegan, B.; Licona, J. C.; Martínez-Ramos, M.; Mazzei, L.; Meave, J.A.; Muñoz, R.; Nytch, C. J.; Oliveira, A. A.; Pérez-García, E. A.; Prado-Junior, J.; Rodríguez-Velázques, J.; Ruschel, A. R.; Salgado-Negret, B.; Schiavini, I.; Swenson, N. G.; Tenorio, E. A.; Thompson, J.; Toledo, M.; Uriarte, M.; van der Hout, P.; Zimmerman, J. K.; Peña-Claros, M. 2018. Biodiversity and climate determine the functioning of Neotropical forests. Global ecology and biogeography, 26, (12), 1423-1434. https://doi.org/10.1111/geb.12721

Powell, S. L.; Cohen, W. B.; Healey, S. P.; Kennedy, R. E.; Moisen, G. G.; Pierce, K. B.; Ohmann, J. L. 2010. Quantification of live aboveground forest biomass dynamics with Landsat time-series and field inventory data: A comparison of empirical modeling approaches. Remote Sensing of Environment, 114, (5), 1053-1068. https://doi.org/10.1016/j.rse.2009.12.018

QGIS. QGIS Development Team. 2021. QGIS Geographic Information System. Open Source Geospatial Found.

R Core Team. 2021. A Language and Environment for Statistical Computing.

Ren, H.; Zhou, G.; Zhang, F. 2018. Using negative soil adjustment factor in soil-adjusted vegetation index (SAVI) for aboveground living biomass estimation in arid grasslands. Remote Sensing of Environment, 209, (2018), 439-445. https://doi.org/10.1016/j.rse.2018.02.068

Riley, S. J.; DeGloria, S. D; Elliot, R. 1999. A terrain ruggedness index that quantifies topographic heterogeneity. Intermountain Journal of Sciences, 5, (1-4), 23-27.

Ripley, B.; Venables, B.; Bates, D. M.; Hornik, K.; Gebhardt, A.; Firth, D.; Ripley, M.B. 2013. Package 'mass'. Cran r. 538:113-120.

Rio de Janeiro. 1991. Lei Estadual n° 1.901, de 29 de novembro de 1991. Dispõe sobre a criação do Parque Estadual da Serra da Tiririca e dá outras providencias.

Rolim, S. G.; Jesus, R. M.; Nascimento, H. E. M.; Couto, H. T. Z.; Chambers, J. C. 2005. Biomass change in an Atlantic tropical moist forest: the ENSO effect in permanent sample plots over a 22-year period. Oecologia, 142, (2005), 238-246. https://doi.org/10.1007/s00442-004-1717-x

Rouse, J. W.; Haas, R. H.; Schell, J. A.; Deering, D. W.; Harlan, J. C. 1973. Monitoring the vernal advancement and retrogradation (green wave effect) of natural vegetation. NASA/GSFC Type III Final Report. Greenbelt. 371p.

Saatchi, S. S.; Houghton, R. A.; Dos Santos Alvala, R. C.; Soares, J. V.; Yu, Y. 2007. Distribution of aboveground live biomass in the Amazon basin. Global change biology, 13, (4), 816-837. https://doi.org/10.1111/j.1365-2486.2007.01323.x

Saatchi, S. S.; Harris, N. L.; Brown, S.; Lefsky, M.; Mitchard, E. T; Salas, W.; Zutta, B. R.; Buermann, W.; Lewis, S. L.; Hagen, S.; Petrova, S.; White, L.; Silman, M.; More, A. 2011a. Benchmark map of forest carbon stocks in tropical regions across three continents. Proceedings of the national academy of sciences, 108, (24), 9899-9904. https://doi.org/10.1073/pnas.101957610

Saatchi, S.; Marlier, M.; Chazdon, R. L.; Clark, D. B.; Russell, A. E. 2011b. Impact of spatial variability of tropical forest structure on radar estimation of aboveground biomass. Remote Sensing of Environment, 115, (11), 2836-2849. https://doi.org/10.1016/j.rse.2010.07.015

Sanchez, M.; Pedroni, F.; Eisenlohr, P. V.; Oliveira-Filho, A. T. 2013. Changes in tree community composition and structure of

Atlantic rain forest on a slope of the Serra do Mar range, southeastern Brazil, from near sea level to 1000 m of altitude. Flora-Morphology, Distribution, Functional Ecology of Plants, 208, (3), 184-196. https://doi.org/10.1016/j.flora.2013.03.002

Santos, E. B.; Pimentel, R. M. M.; Silva, M. D. 2023. Landscape Ecology applied to the study of the Atlantic Forest. Journal of Environmental Analysis and Progress, 8, (3), 184-189. https://doi.org/10.24221/jeap.8.3.2023.5427.184-189

Sakate, D. M.; Kashid, D. N. 2014. A deviance-based criterion for model selection in GLM. Statistics, 48, (1), 34-48. https://doi.org/10.1080/02331888.2012.708035

Sampaio, T. V. M.; Augustin, C. H. R. R. 2014. Índice de concentração da rugosidade: uma nova proposta metodológica para o mapeamento e quantificação da dissecação do relevo como subsídio a cartografia geomorfológica. Revista Brasileira de Geomorfologia, 15, (1), 47-60. https://doi.org/10.20502/rbg.v15i1.376

Silva, L. C.; Araújo, E. J. G.; Curto, R. A.; Nascimento, A. M.; Ataíde, D. H. dos S.; Morais, V. A. 2018. Estoques de biomassa e carbono em unidade de conservação no Bioma Mata Atlântica. BIOFIX Scientific Journal, 3, (2), 243-251. https://dx.doi.org/10.5380/biofix.v3i2.59592

Schuh, M.; Favarin, J. A. S.; Marchesan, J.; Alba E.; Berra, E. F.; Pereira, R. S. 2020. Machine learning and generalized linear model techniques to predict aboveground biomass in Amazon rainforest using LiDAR data. Journal of Applied Remote Sensing, 14, (3), 034518. https://doi.org/10.1117/1.JRS.14.034518

Shepard, D. 1968. A two-dimensional interpolation function for irregularly-spaced data. In: Proceedings of the 1968 23rd ACM national conference. pp. 517-524.

Silveira, E. M. D. O.; Cunha, L. I. F.; Galvão, L. S.; Withey, K. D.; Acerbi Júnior, F. W.; Scolforo, J. R. S. 2019. Modelling aboveground biomass in forest remnants of the Brazilian Atlantic Forest using remote sensing, environmental and terrain-related data. Geocarto International, 36, (3):281-298. https://doi.org/10.1080/10106049.2019.1594394

SOS Mata Atlântica; INPE. 2019. Relatório anual 2019. 29p.

Timothy, D.; Onisimo, M.; Cletah, S.; Adelabu, S.; Tsistsi, B. 2016. Remote sensing of aboveground forest biomass: A review. Tropical Ecology, 57, (2), 125-132.

Toledo, R. M.; Santos, R. F.; Baeten, L.; Perring, M. P.; Verheyen, K. 2018. Soil properties and neighbouring forest cover affect aboveground biomass and functional composition during tropical forest restoration. Applied Vegetation Science, 21, (2), 179-189. https://doi.org/10.1111/avsc.12363

Vieira, S. A.; Alves, L. F.; Duarte-Neto, P. J.; Martins, S. C.; Veiga, L. G.; Scaranello, M. A.; Picollo, M. C.; Camargo, P. B.; Carmo, J. B.; Sousa Neto, E.; Santos, F. A. M.; Joly, C. A.; Martinelli, L. A. 2011. Stocks of carbon and nitrogen and partitioning between above-and belowground pools in the Brazilian coastal Atlantic Forest elevation range. Ecology and Evolution, 1, (3), 421-434. https://doi.org/10.1002/ece3.41

Wilson, J. P.; Gallant, J. C. 2000. Book Review Terrain Analysis: Principles and Applications. Ecology Eng. John Wiley & Sons, Inc. vol. 18, pp. 121-122.

Xavier, A. C.; Vettorazzi, C. A. 2004. Mapping leaf area index through spectral vegetation indices in a subtropical watershed. International Journal of Remote Sensing, 25, (9), 1661-1672. https://doi.org/10.1080/01431160310001620803

Zhu, X.; Liu, D. 2015. Improving forest aboveground biomass estimation using seasonal Landsat NDVI time-series. ISPRS Journal of Photogrammetry and Remote Sensing, 102, (2015), 222-231. https://doi.org/10.1016/j.isprsjprs.2014.08.014

Zuñe-da-Silva, F.; Rodrigues, P. J. F. P., Rojas-Idrogo, C.; Delgado-Paredes, G. E.; Enrich-Prast, A.; Sakuragui, C. M. 2023. Tree structure and composition of a coastal remnant of the Atlantic Forest in Rio de Janeiro. Advances in Forestry Science, 10, (1), 1929-1940. https://doi.org/10.34062/afs.v10i1.13347